0026-895X/08/7406-1485–1495$20.00
MOLECULAR PHARMACOLOGY
Copyright © 2008 The American Society for Pharmacology and Experimental Therapeutics
*Mol Pharmacol* 74:1485–1495, 2008

Vol. 74, No. 6
49775/3404399
*Printed in U.S.A.*



# Comparison of the Potential Multiple Binding Modes of Bicyclam, Monocylam, and Noncyclam Small-Molecule CXC Chemokine Receptor 4 Inhibitors

Rebecca S. Y. Wong, Veronique Bodart, Markus Metz, Jean Labrecque, Gary Bridger, and Simon P. Fricker

*Genzyme Corporation, Cambridge, Massachusetts*

Received June 17, 2008; accepted September 2, 2008

## ABSTRACT

CXC chemokine receptor (CXCR)4 is an HIV coreceptor and a chemokine receptor that plays an important role in several physiological and pathological processes, including hematopoiesis, leukocyte homing and trafficking, metastasis, and angiogenesis. This receptor belongs to the class A family of G protein-coupled receptors and is a validated target for the development of a new class of antiretroviral therapeutics. This study compares the interactions of three structurally diverse small-molecule CXCR4 inhibitors with the receptor and is the first report of the molecular interactions of the nonmacrocyclic CXCR4 inhibitor (*S*)-*N*′-(1*H*-benzimidazol-2-ylmethyl)-*N*′-(5,6,7,8-tetrahydroquinolin-8-yl)butene-1,4-diamine (AMD11070). Fourteen CXCR4 single-site mutants representing amino acid residues that span the entire putative ligand binding pocket were used in this study. These mutants were used in binding studies to examine how each single-site mutation affected the ability of the inhibitors to compete with $^{125}$I-stromal-derived factor-1$\alpha$ binding. Our data suggest that these CXCR4 inhibitors bind to overlapping but not identical amino acid residues in the transmembrane regions of the receptor. In addition, our results identified amino acid residues that are involved in unique interactions with two of the CXCR4 inhibitors studied. These data suggest an extended binding pocket in the transmembrane regions close to the second extracellular loop of the receptor. Based on site-directed mutagenesis and molecular modeling, several potential binding modes were proposed for each inhibitor. These mechanistic studies might prove to be useful for the development of future generations of CXCR4 inhibitors with improved clinical pharmacology and safety profiles.

CXCR4 is a chemokine receptor and a coreceptor for T-tropic (CXCR4-using) HIV viruses. The developments of drug resistance and toxicities in the current drug classes have prompted the investigation into novel antiretroviral agents with unique targets of action. Inhibition of viral entry by coreceptor blockade has been a target under active investigation (Moore and Doms, 2003).

CXCR4 belongs to the class A family of seven transmembrane G protein-coupled receptors (GPCRs), which also includes a significant portion of proven drug targets (Klabunde and Hessler, 2002). CXCR4 is expressed on a multitude of tissues and cell types and has been shown to be involved in the homing and trafficking of leukocytes and hematopoietic progenitor cells, brain development, vascularization, neonatal development, T-cell activation and migration at sites of inflammation, and hematopoiesis (Murdoch, 2000). SDF-1 (also known as CXCL12) is the only known ligand that binds to CXCR4. In addition to its physiological roles, the SDF-1$\alpha$-CXCR4 axis has been suggested to play an important role in the progression of different types of cancer, including breast cancer, small cell lung cancer, chronic lymphocytic leukemia, and neuroblastoma (Burger and Kipps, 2006),. The effects of the SDF-1$\alpha$-CXCR4 axis on tumor progression are thought to be mediated through a combination of promoting tumor cell survival, metastasis, and/or angiogenesis. The blockade of CXCR4, either by neutralizing antibody or small-molecule inhibitor, has been shown to have antimetastatic effects on many cancers (Burger and Kipps, 2006).

AMD3100 (plerixafor) is the first nonpeptide, small-molecule CXCR4 inhibitor reported in the literature (Bridger et al., 1995). Clinical studies of AMD3100 in HIV-infected patients have provided proof of concept for CXCR4 blockade in HIV therapy (Hendrix et al., 2004). AMD3100 is currently

Article, publication date, and citation information can be found at http://molpharm.aspetjournals.org.
doi:10.1124/mol.108.049775.

**ABBREVIATIONS:** CXCR, CXC chemokine receptor; GPCR, G protein coupled receptor; SDF-1, stromal-derived factor-1; h, human; FBS, fetal bovine serum; DMEM, Dulbecco's modified Eagle's medium; CHO, Chinese hamster ovary; ECL, extracellular loop; TM, transmembrane; AMD11070, (*S*)-*N*′-(1*H*-benzimidazol-2-ylmethyl)-*N*′-(5,6,7,8-tetrahydroquinolin-8-yl)butane-1,4-diamine.

in late-stage clinical trials as a stem colony mobilization agentin combination with granulocyte colony-stimulating factor (Flomenberg et al., 2005). AMD3465 is a monocyclam CXCR4 inhibitor with reduced molecular size and charge compared with AMD3100 (Hatse et al., 2005). In addition to its antiviral activity, a recent report has shown that it could abrogate T-helper 2-mediated hypersensitivity-type inflammation, indicating a potential application of CXCR4 antagonism for the treatment of chronic hypersensitivity diseases (Hu et al., 2006). AMD11070 is the first orally bioavailable small-molecule CXCR4 inhibitor. In a phase Ib/IIa dose-escalating proof-of-concept clinical study for the treatment of HIV-infected patients carrying X4-using viruses, AMD11070 demonstrated activity in the first dose cohort (Moyle et al., 2007; Saag et al., 2007).

The evolution from the macrocyclic and positively charged AMD3100 to the monocyclam AMD3465 and to the noncyclam AMD11070 not only represents a progressive reduction in both molecular size and charge but also, more importantly, the gain of oral bioavailability. All three compounds have been shown to bind to CXCR4 in a specific and reversible manner, with no cross-reactivity with other chemokine receptors, including CCR1, CCR2b, CCR4, CCR5, CCR7, and CXCR3 (Schols et al., 2003; Hatse et al., 2005; Fricker et al., 2006). In addition, they have been shown to inhibit SDF-1$\alpha$ ligand binding to CXCR4, and SDF-1$\alpha$-mediated calcium flux, G protein activation, chemotaxis, and receptor internalization, as well as the SDF-1$\alpha$-independent viral replication of T-tropic HIV viruses. Because all three compounds are structurally diverse yet demonstrate similar patterns of CXCR4 inhibitory activity, it is of interest to examine their modes of interaction with the receptor.

An interesting structural feature of the bicyclam molecule AMD3100 is the four protonated nitrogens (two per cyclam ring) present at physiological pH. This suggests the possibility for interactions with negatively charged amino acids such as aspartate and glutamate. This has been demonstrated in a series of elegant experiments (Gerlach et al., 2001; Hatse et al., 2001; Rosenkilde et al., 2004). In this study, we compare and investigate the binding modes of the bicyclam AMD3100, the monocyclam AMD3465, and the noncyclam AMD11070. We used site-directed mutagenesis to generate single-site mutants of the cloned human CXCR4 (hCXCR4) gene. The mutants were used to investigate how each selected amino acid affected the ability of the inhibitors to compete with $^{125}$I-SDF-1$\alpha$ binding to the receptor. Taking these experimental data into account, molecular modeling was used to dock these inhibitors into the receptor to suggest the possible binding modes of these structurally diverse compounds. Based on the data from these studies, we propose that each molecule has the potential to bind in more than one mode to the CXCR4 receptor. Understanding the interactions between the receptor and its inhibitors will probably assist in the development of future generation therapeutics with different resistance profiles and improved pharmacological and safety properties.

## Materials and Methods

**Cell Lines and Reagents.** All compounds were chemically synthesized at AnorMED as described previously (Bridges et al., 1995; Hatse et al., 2005). SDF-1$\alpha$ was provided by the late I. Clarke Lewis (University of British Columbia, Vancouver, BC, Canada). $^{125}$I-SDF-1$\alpha$ was purchased from PerkinElmer Life and Analytical sciences (Boston, MA). Cell culture media and reagents were purchased from Invitrogen (Carlsbad, CA).

CCRF-CEM cell line (CCL-119), which endogenously expresses hCXCR4, was obtained from American Type Culture Collection (Manassas, VA) and maintained in RPMI 1640 medium containing 1 mM sodium pyruvate, 2 mM L-glutamine, and 10% FBS. P4-R5 MAGI cells and pDOLHIVenv plasmid were obtained through the AIDS Research and Reference Reagent Program (Division of AIDS, National Institute of Allergy and Infectious Diseases, National Institutes of Health, Bethesda, MD): pDOLHIVenv from Drs. Eric Freed and Rex Risser (Freed et al., 1989). P4-R5 MAGI cells were maintained in DMEM, 10% FBS, supplemented with 1 $\mu$g/ml puromycin. CHO-K1 cells were maintained in F-12 K media with 10% FBS. Canine thymus (Cf2Th) cells were obtained from American Type Culture Collection and maintained in DMEM containing 1 mM sodium pyruvate, 4 mM L-glutamine, and 20% FBS.

**Site-Directed Mutagenesis of hCXCR4 cDNA.** CXCR4 single-site mutants were generated by site-directed mutagenesis of the cloned hCXCR4 in pcDNA3.1 using the QuikChange mutagenesis kit following the supplier's protocol (Stratagene, La Jolla, CA). Mutagenesis primers were purchased from Operon Biotechnologies (Huntsville, AL). DNA sequencing was performed on all the mutants to confirm that the target sequence was obtained. DNA sequencing was performed by the Nucleic Acid Protein Service Unit at the University of British Columbia. Mutants D171N, V196A, D262N, H281A, and E288A were obtained from M. Rosenkilde and T. Schwartz (Panum Institute, Copenhagen University, Copenhagen, Denmark).

**CXCR4-Mediated Cell Fusion.** Plasmid pDOLHIVenv contains a 3108-base pair SalI-XhoI fragment encompassing the open reading frames of the *env*, *tat*, *rev* coding regions from pNL4-3. P4-R5 MAGI cells express endogenous CD4 and CXCR4 on the cell surface and have also been stably transformed with a $\beta$-galactosidase that is under the control of HIV-long terminal repeat, which is transactivated by HIV or simian immunodeficiency virus Tat protein. CHO-K1 cells (>95% confluent) were transiently transfected with endotoxin-free preparation of the plasmid pDOLHIVenv using Lipofectamine 2000 accordingly to supplier's protocol (Invitrogen). Twenty-four hours after the transfection, cells were lifted and resuspended at $4 \times 10^5$ cells/ml and mixed with P4-R5 MAGI cells (1:1 ratio) in white 96-well plates in the presence of CXCR4 inhibitors. Cells were incubated for 16 to 20 h at 37°C, 5% $CO_2$. Interaction of CXCR4 expressed on P4-R5 MAGI cells and gp120 on the transiently transfected CHO-K1 cells induced fusion of the two cell types and resulted in the transactivation of the $\beta$-galactosidase gene. Fusion level was monitored using the Galscreen substrate (Applied Biosystems, Foster City, CA), with luminescence measured by Victor2 spectrophotometer (PerkinElmer Wallac, Gaithersburg, MD). $IC_{50}$ values were calculated using Prism 4.0 software (GraphPad Software Inc., San Diego, CA).

**$^{125}$I-SDF-1$\alpha$ Competitive Binding.** Competitive binding studies for hCXCR4 were performed in either CCRF-CEM cells or Cf2Th cells transiently transfected with hCXCR4 cDNA. Expression of hCXCR4 was confirmed by flow cytometry using a fluorescein isothiocyanate-labeled anti-CXCR4 antibody, 12G5 (R&D Systems, Minneapolis, MN). A concentration range of CXCR4 inhibitors was incubated for 3 h at 4°C in binding buffer (phosphate-buffered saline containing 5 mM $MgCl_2$, 1 mM $CaCl_2$, and 0.25% bovine serum albumin, pH 7.4) with $5 \times 10^5$ cells and 100 pM $^{125}$I-SDF-1$\alpha$ (2200 Ci/mmol; PerkinElmer Life and Analytical sciences) in Durapore filter plates (Millipore Corporation, Billerica, MA). Unbound $^{125}$I-SDF-1$\alpha$ was removed by washing with 50 mM HEPES and 0.5 M NaCl, pH 7.0, at 4°C. The bound radioactivity was counted using a 1450 MicroBeta liquid scintillation counter (PerkinElmer Wallac). The data were analyzed by nonlinear regression using Prism 4.0 software (GraphPad Software Inc.). In most cases, binding studies

with Cf2Th cells transiently transfected with mutant hCXCR4 were performed at least twice. Wild-type hCXCR4 was included as a comparative control in all experiments. In all cases, there was <3-fold difference in replicates.

**Calcium Flux Signaling Experiments.** The potency of the CXCR4 inhibitors was examined in calcium flux signaling assays. CCRF-CEM cells were resuspended ($7 \times 10^6$ cells/ml) in serum-reduced media (RPMI 1640 medium containing 2% FBS) and loaded with the ester form of the calcium indicator, Fluo-4 (1 $\mu$M; Invitrogen), for 30 min at 37°C. The dye-loaded cells were washed twice with Hanks' balanced salt solution containing 20 mM HEPES, 0.2% bovine serum albumin, and 2.5 mM probenecid, pH 7.4. The cells were resuspended in the same buffer ($7 \times 10^6$ cells/ml) followed by a 20-min incubation at room temperature in the dark. The cells were then incubated in the dark at 37°C for 15 min with CXCR4 inhibitors. Changes in intracellular calcium concentration upon SDF-1$\alpha$ addition (15 nM) were monitored using the FLEXstation (Molecular Devices, Sunnyvale, CA) at 525 nm (excitation $\lambda$, 485 nm). The fluorescence data were analyzed using the program Softmax PRO 4.0 (Molecular Devices), and $EC_{50}$ values were calculated using Prism 4.0 software (GraphPad Software Inc.).

To examine the calcium signaling of the mutated hCXCR4, Cf2Th cells (70–90% confluent) were transiently transfected with the cloned cDNAs of mutated CXCR4 and chimeric G protein $G_{qi5}$ using Lipofectamine 2000 (Invitrogen). Forty-eight hours after transfection, Cf2Th cells were resuspended ($1 \times 10^7$ cells/ml) in serum-reduced media (DMEM and 2% FBS) and loaded with the ester form of the calcium indicator Fluo-4 (4 $\mu$M) as indicated above. After washing, cells were resuspended at $4 \times 10^6$ cells/ml and incubated for 15 min in the dark at 37°C with CXCR4 inhibitors. Changes in intracellular calcium concentration upon SDF-1$\alpha$ addition were monitored using the FLEXstation and analyzed by Prism 4.0 software (GraphPad Software Inc.) as described above.

**Molecular Modeling.** Modeler within Insight2000.1 (Accelrys, San Diego, CA) was used to generate the CXCR4 homology model. Bovine rhodopsin (1HZX.pdb) was used as the template (Teller et al., 2001). The alignment followed general rules for GPCRs to allow no gaps in the helix regions as well as to align residues conserved across most of the GPCR class A family (Onuffer and Horuk, 2002). The extracellular loops (ECLs) and intracellular loops were not included. Several models of CXCR4 were generated, and the model with the lowest probability density function value and energy was used for further geometry optimizations during which the helical C$\alpha$ coordinates of the transmembrane region of CXCR4 were kept fixed to keep the helices position as closely as possible to the crystal coordinates of bovine rhodopsin (Oliveira et al., 2004). Nevertheless, the region of helix II close to the extracellular region had to be adjusted. CXCR4 has in this region a TXP motif compared with the GGF motif of bovine rhodopsin. To accommodate this change, the procedure described in Paterlini (2002) was used. The Ramachandran plot of the final homology model shows all of the residues in the allowed region. The structures of the CXCR4 inhibitors included in this study (Fig. 1) were generated with Insight2000.1 and subjected to energy minimization with Discover module (Accelrys, San Diego, CA). The structures were manually docked into the CXCR4 receptor model based upon the experimental data from the CXCR4 mutants/inhibitors binding studies, followed by geometry optimizations with Discover keeping backbone atoms of the transmembrane region of the receptor fixed. In addition, MOE2005.06 (Chemical Computing Group, Montreal, QC, Canada) was used to manually dock the inhibitors into the binding site of the CXCR4 homology model in order to explain CXCR4 mutants/inhibitors binding data. The ligand-receptor complexes were geometrically optimized with the MMFF94x force field within MOE software system. Likewise, backbone atoms of the transmembrane region of the receptor were kept rigid during geometry optimizations.

## Results

**Characterization of CXCR4 Inhibitors.** AMD3100 and AMD3465 have been described previously (Bridger et al., 1995; Hatse et al., 2005; Fricker et al., 2006). AMD11070 was discovered during the AnorMED in-house CXCR4 inhibitor drug research and discovery program to develop an orally bioavailable compound (Schols et al., 2003). The chemical structures of these inhibitors are shown in Fig. 1. All compounds were potent inhibitors of CXCR4-mediated cell fusion (Fig. 2) and demonstrated inhibitory effects on $^{125}$I-SDF-1$\alpha$ binding (Fig. 3) and SDF-1$\alpha$-induced calcium flux in CCRF-CEM cells (Table 1). The $IC_{50}$ rankings of the three inhibitors are the same in $^{125}$I-SDF-1$\alpha$ competitive binding assay and SDF-1$\alpha$-induced calcium flux signaling using the CXCR4 receptor expressed endogenously on CCRF-CEM cells. The $IC_{50}$ values of AMD3100 were ~600 nM in these two assays, whereas those of AMD3465 and AMD11070 were ~10 to 40 nM and ~10 nM, respectively. It is noteworthy that although AMD3100 was >10-fold less potent than the other two compounds in the inhibition of calcium flux signaling and $^{125}$I-SDF-1$\alpha$ binding, it was as effective in anti-cell fusion activity as these inhibitors, with an $IC_{50}$ value in the nanomolar range. All these compounds have been shown to have antiviral activity in the 1 to 10 nM range (Schols et al., 2003; Hatse et al., 2005). The wide range in inhibitory potency of AMD3100 in different assays has been observed previously (Fricker et al., 2006). Possible explanations are differences in

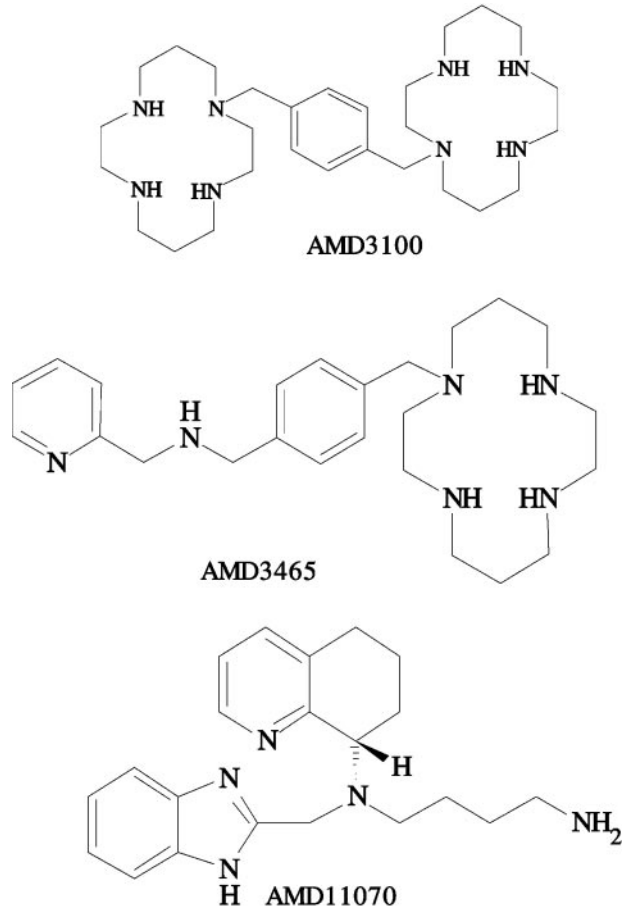


**Fig. 1.** Chemical structures of CXCR4 inhibitors; for docking, the protonation states have been adjusted to pH 7.0.

cell type, experimental conditions, and divergent signaling pathways for different receptor-mediated events. An alternative, and more likely, explanation for the differences in activity observed between these assays may also be in part due to the tight binding of AMD3100 to CXCR4, and to the differences in the relative time course of the different assays. This is supported by previously reported studies from our laboratory investigating the time course of compound/receptor association and dissociation (Fricker et al., 2006).

**Site-Directed Mutagenesis of CXCR4 Receptor.** Because the three CXCR4 inhibitors are structurally diverse and seem to exhibit similar but distinct profiles of inhibition on calcium flux signaling, $^{125}$I-SDF-1$\alpha$ competitive binding, and cell fusion, it was of interest to study their interactions with the CXCR4 receptor at the molecular level. Nine single-site mutants spanning the entire putative small-molecule inhibitor binding site of CXCR4 receptor were generated in this study. In addition to the five single-site mutants kindly provided by M. Rosenkilde and T. Schwartz, a total of 14 mutants were used for the investigation. Figure 4 shows the amino acid sequence alignment of human CXCR4 with the other chemokine receptors and indicates the residues mutated in this study.

**Characterizations of CXCR4 Single-Site Mutants.** The Cf2Th cell line was used for the expression of the CXCR4 mutants because this cell line did not show any significant background CXCR4 activity in SDF-1$\alpha$ binding and SDF-1$\alpha$-induced calcium flux signaling experiments (data not shown). All three inhibitors exhibited very similar $IC_{50}$ values in the SDF-1$\alpha$ competitive binding assay conducted in the recombinant Cf2Th system using wild-type hCXCR4 (Table 3), and they showed the same ranking of inhibitor activity compared with the CCRF-CEM cell line, suggesting that the conformation of the recombinant wild-type hCXCR4 expressed in Cf2Th cells is similar to that of the endogenous CXCR4 in CCRF-CEM cells (Table 1).

Expression of each mutant hCXCR4 was confirmed qualitatively by flow cytometry; however, because of the inherent nature of the transient transfection, the signal was low, thereby not allowing for quantitative comparisons with this technique. The relative expression of the mutant hCXCR4 with wild-type receptor after transient transfection was evaluated by comparing the $B_{max}$ of the mutant receptor with the $B_{max}$ of the wild-type receptor control performed for the respective mutant. The expression of six of the mutants, N176A, R183A, V196A, H203A, and Y255A, were similar to the wild type (≥80%); Y45A, D97N, and Y121A were expressed at a slightly lower level (60–80%); and W94A, D171N, D262N, and E288A exhibited consistent low expression (<50%), whereas Y116A and H281A were overexpressed compared with the wild-type receptor (Table 2).

The single mutants were characterized in terms of their affinity and response to SDF-1$\alpha$. Table 2 summarizes the SDF-1$\alpha$ binding $K_d$ values and calcium flux signaling $EC_{50}$ values of the mutants. Receptor expression was confirmed by $^{125}$I-SDF-1$\alpha$ binding. The $^{125}$I-SDF-1$\alpha$ binding $K_d$ values of the mutants ranged from 6.9 to 86.2 nM (wild-type $K_d$ = 35.8 nM). The SDF-1$\alpha$ $EC_{50}$ value in calcium flux signaling of the mutants ranged from 26.1 to 138.2 nM (wild-type $EC_{50}$ = 34 nM). The SDF-1$\alpha$ $EC_{50}$ values in calcium flux signaling and $K_d$ values in homologous competitive binding of these mutants were within 3- to 4-fold compared with those of the wild-type receptor. The findings that all these mutants demonstrated close to wild-type $K_d$ values in the binding assay indicate that the mutations did not significantly alter the conformation of the receptor.

The maximal signaling response of the mutants was measured by monitoring the intracellular calcium flux in response to 200 nM SDF-1$\alpha$, a concentration that is >5-fold higher than the $EC_{50}$ value (34 nM) obtained in our laboratory. Seven mutants showed >60% of the wild-type signaling response at 200 nM SDF-1$\alpha$, four mutants showed ~20 to 40% response, and three mutants (D97N, Y116A, and E288A) showed no response to SDF-1$\alpha$.

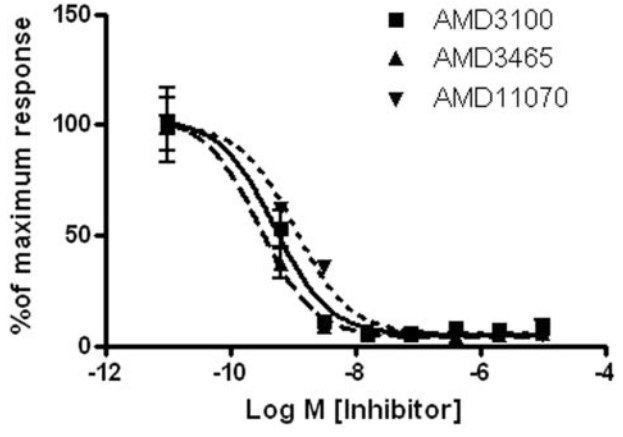


**Fig. 2.** Inhibitory effect of CXCR4 inhibitors on CXCR4-mediated cell fusion.

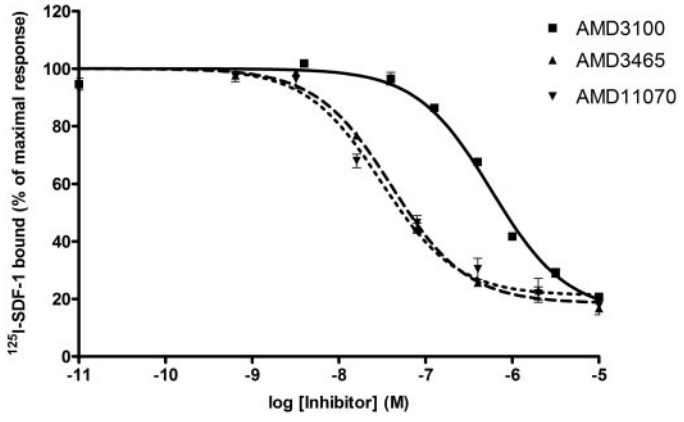


**Fig. 3.** Competitive binding curves of CXCR4 inhibitors for the binding of $^{125}$I-SDF-1$\alpha$ on wild-type CXCR4 expressed endogenously in CCRF-CEM cells.

TABLE 1
Inhibition of $^{125}$I-SDF-1$\alpha$ binding, SDF-1$\alpha$-induced calcium mobilization in CEM cells, and CXCR4-mediated cell fusion by CXCR4 inhibitors
Results are expressed as mean ± S.E.

| | $IC_{50}$ | | |
|---|---|---|---|
| | $^{125}$I-SDF-1$\alpha$ Binding | SDF-1$\alpha$-Induced Calcium Flux | CXCR4-Mediated Cell Fusion |
| | *nM* | | |
| AMD3100 | 651.0 ± 37.0 | 572.0 ± 190 | 0.9 ± 0.5 |
| AMD3465 | 41.7 ± 1.2 | 12.1 ± 2.4 | 0.4 ± 0.2 |
| AMD11070 | 12.5 ± 1.3 | 9.0 ± 2.0 | 1.5 ± 0.3 |

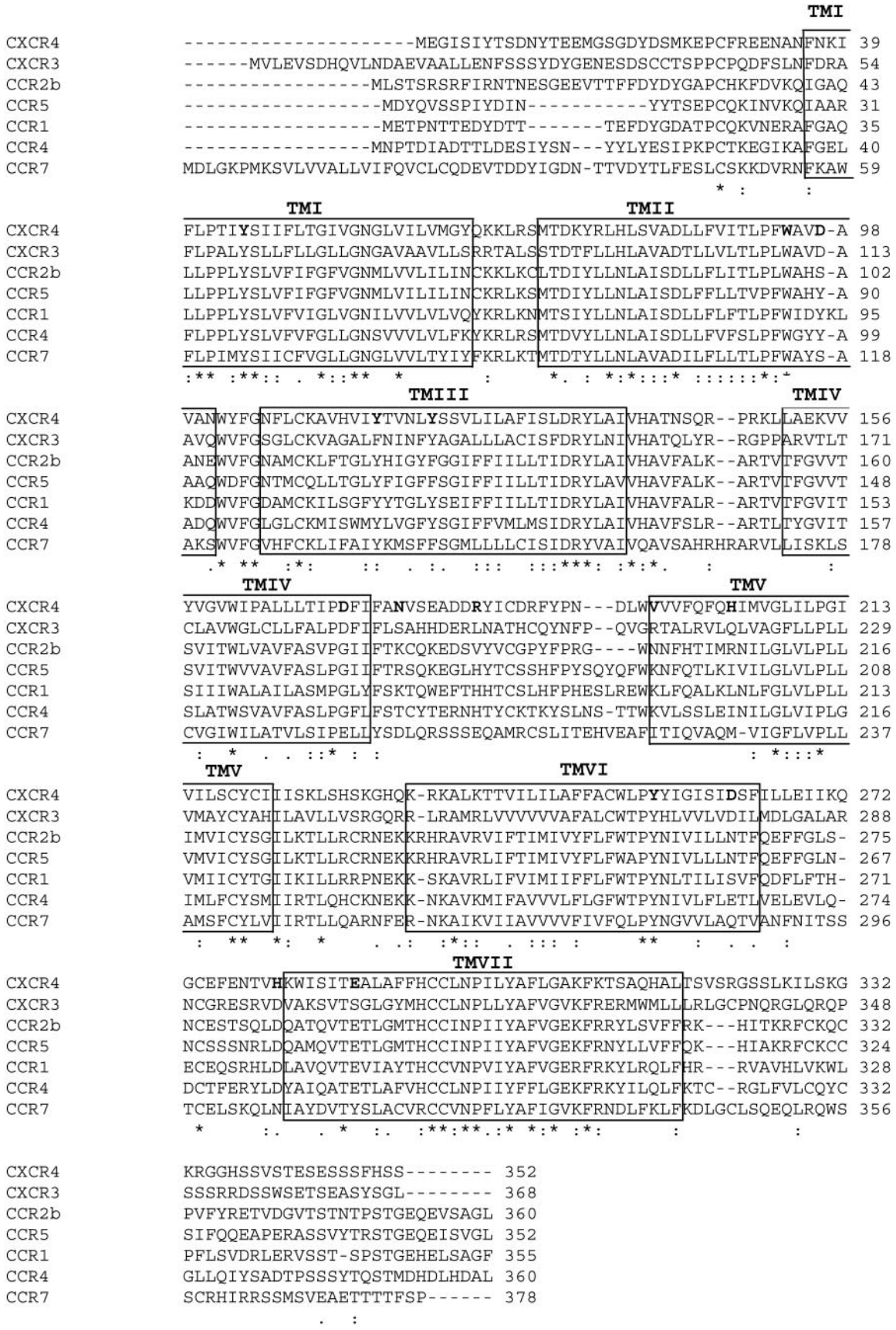


**Fig. 4.** Amino acid sequence alignment of CXCR4 with other human chemokine receptors. The alignment was performed with CLUSTALW (1.83). The amino acids changed by site-directed mutagenesis are indicated in bold. Transmembrane segments are assigned as predicted by TMPred. The coding regions of the nucleotide sequences with the following accession numbers were used: CXCR4 (AF005058) (Wegner et al., 1998), CXCR3 (U32674) (Marchese et al., 1995), CCR2b (U80924) (Wong et al., 1997), CCR5 (NM_000579) (Brands et al., 1986), CCR1 (NM_001295) (Neote et al., 1993), CCR4 (X85740) (Power et al., 1995), and CCR7 (NM_001838) (Birkenbach et al., 1993).

**Effects of Single-Site Mutations on Inhibitor Affinity for the CXCR4 Receptor.** The effects of CXCR4 single-site mutations on inhibitor binding were examined by $^{125}$I-SDF-1$\alpha$ competitive binding with CXCR4 inhibitors (Table 3). Each of the three inhibitors was affected differently by the single mutations. For AMD3100, E288A mutant affected the $K_i$ value most severely, increasing it by 35-fold compared with that of the wild type (0.84 $\mu$M versus 29.4 $\mu$M). Mutations Y45A, W94A, Y116A, D171N, and D262N all resulted in ~10- to 20-fold increase in $K_i$ values. For AMD3465, mutations D262N and H281A increased the $K_i$ values by >100-fold; mutations W94A and E288A increased the $K_i$ values by 50- to 100-fold; and mutations Y45A, Y116A, and D171N affected the $K_i$ values by ~10- to 30-fold. For AMD11070, four mutations (W94A, D97N, D171N, and E288A) increased the $K_i$ values of AMD11070 by >100-fold, whereas 2 of them (Y45A and D262N) increased the $K_i$ values by 10- to 50-fold.

Among all mutations, Y45A, W94A, D171N, D262N, and E288A, affected the $K_i$ values of all three inhibitors, although by different degrees. D97N and H281A affected only the binding of AMD11070 and AMD3465, respectively. One mutation in TMIII (Y121A), all three mutations studied in the ECLII (N176A, R183A, and V196A), and one mutation each in TMV and TMVI (H203A and Y255A, respectively), had no significant impact (<5-fold) on the binding of the inhibitors. Figure 5 shows a schematic diagram of the receptor depicting the approximate positions of the mutated amino acids in the transmembrane segments, with the mutated amino acids coded in different colors according to their effects on the affinity of the inhibitors.

**Interactions of Small-Molecule CXCR4 Inhibitors with hCXCR4 Based on Molecular Modeling.** Based on experimental results presented here, acidic amino acids (Asp$^{97}$, Asp$^{171}$, Asp$^{262}$, and Glu$^{288}$) have been used as "anchor points" to determine potential binding modes for the small-molecule inhibitors. Each compound has been docked into the small-molecule binding site to enable some of these ionic H-bond interactions while trying to explain as many additional mutant $K_i$ -fold changes as possible. It should be noted that none of the binding modes could account for all of the amino acid residues that have been shown to affect the binding of the inhibitors. To accommodate all the amino acid residues indicated by the mu-

TABLE 2
Characterization of hCXCR4 mutants by $^{125}$I-SDF-1$\alpha$ binding and SDF-1$\alpha$-induced calcium flux signaling in transfected Cf2Th cells

| | $^{125}$I-SDF-1$\alpha$ Binding $K_d$ | Mean Relative $B_{max}$[a] ± S.D. | SDF-1$\alpha$ Calcium Flux Signaling $EC_{50}$ | Wild-Type Response in Presence of 200 nM SDF-1$\alpha$ |
|---|---|---|---|---|
| | *nM* | % | *nM* | % |
| WT | 35.8 | 100 | 34.0 | 100 |
| Y45A | 22.8 | 70.8 ± 3.7 | 33.9 | 25.6 |
| W94A | 54.9 | 43.4 ± 2.8 | 45 | 19.8 |
| D97N | 47.6 | 72.6 ± 24.8 | N.R. | N.R. |
| Y116A | 33.7 | 170.7 ± 7.9 | N.R. | N.R. |
| Y121A | 86.2 | 58.4 | 100 | 64.9 |
| D171N | 73.6 | 39.7 ± 1.1 | 137.9 | 60.1 |
| N176A | 15.1 | 80.8 ± 26.7 | 59.4 | 68.0 |
| R183A | 16.4 | 79.2 ± 20.7 | 42.9 | 71.6 |
| V196A | 22.7 | 89.2 ± 8.7 | 138.2 | 105.6 |
| H203A | 42.3 | 97.9 ± 22.9 | 26.1 | 103.8 |
| Y255A | 11.8 | 96.7 ± 3.3 | 42.0 | 41.3 |
| D262N | 80.3 | 32.5 ± 2.1 | 96.5 | 60.0 |
| H281A | 6.9 | 133.2 ± 10.0 | 136.3 | 18.5 |
| E288A | 44.1 | 53.1 | N.R. | N.R. |

N.R., no response.
[a] The relative percentage $B_{max}$ = $B_{max}$ in cpm of the mutant/wild type in the same experiment.

TABLE 3
Effects of CXCR4 single-site mutations on $^{125}$I-SDF-1$\alpha$ competitive binding $K_i$ of CXCR4 inhibitors

| | Location | $^{125}$I-SDF-1$\alpha$ $K_i$ of Inhibitors [-Fold Increase Compared with Wild Type] | | | | | |
|---|---|---|---|---|---|---|---|
| | | AMD3100 | | AMD3465 | | AMD11070 | |
| | | *nM* | | *nM* | | *nM* | |
| Wild type | | 842 | [1] | 49 | [1] | 11 | [1] |
| Y45A | TMI | 8465 | [10.0] | 1069 | [21.6] | 438 | [39.8] |
| W94A | TMII | 11,800 | [14.0] | 4437 | [89.5] | 1185 | [107.5] |
| D97N | TMII | 2950 | [3.5] | 176 | [3.6] | 3185 | [289.0] |
| Y116A | TMIII | 8099 | [9.6] | 777 | [15.7] | 39 | [3.5] |
| Y121A | TMIII | 401 | [0.5] | 17 | [0.3] | 19 | [1.7] |
| D171N | TMIV | 9584 | [11.4] | 1350 | [27.2] | 13,760 | [1248.6] |
| N176A | ECLII | 723 | [0.9] | 59 | [1.2] | 8 | [0.8] |
| R183A | ECLII | 501 | [0.9] | 52 | [0.9] | 15 | [0.14] |
| V196A | ECLII | 1205 | [1.4] | 124 | [2.5] | 28 | [2.5] |
| H203A | TMV | 484 | [0.6] | 31 | [0.6] | 9 | [0.9] |
| Y255A | TMVI | 2390 | [2.8] | 225 | [4.5] | 13 | [1.2] |
| D262N | TMVI | 15,030 | [17.8] | 8524 | [172.0] | 137 | [12.5] |
| H281A | TMVII | 137 | [0.2] | 6514 | [131.4] | 24 | [2.2] |
| E288A | TMVII | 29,445 | [35.0] | 3404 | [68.7] | 5073 | [460.3] |

tational analysis we explored optional binding modes for each molecule. Three of the potential binding modes for each small-molecule inhibitor are shown in Fig. 6.

One of the binding modes of AMD3100 closely resembles the binding mode proposed previously (Gerlach et al., 2001; Rosenkilde et al., 2004) (Fig. 6A). In this binding mode, the inhibitor covers the area surrounded by the TMIII, IV, V, VI, and VII and forms ionic hydrogen bond interactions with $Asp^{171}$, $Asp^{262}$, and $Glu^{288}$ simultaneously. Figure 6, B and C, depict two more potential binding modes, which further extend into the TMI, TMII, and TMVII regions. In both binding modes one of the double protonated cyclam rings potentially forms a cationic $\pi$-interaction with the aromatic side chain of $Trp^{94}$ and a hydrogen bond interaction with $Tyr^{45}$. In the second binding mode (Fig. 6B), the second cyclam ring uses $Asp^{171}$ as an interaction site. In the third binding mode (Fig. 6C), a $\pi$-stacking interaction between the phenyl spacer and $Tyr^{116}$ is suggested, whereas the second cyclam ring is able to form an ionic hydrogen bond interaction with $Asp^{262}$. All three binding modes suggest indirect interactions between AMD3100 and some mutated amino acid residues of the receptor.

Likewise, the monocyclam AMD3465 has been docked into the binding site of CXCR4 in several ways (Fig. 6, D–F). For this compound, emphasis has been put on demonstrating a potential aromatic interaction between $His^{281}$ and the pyridine ring. Con-

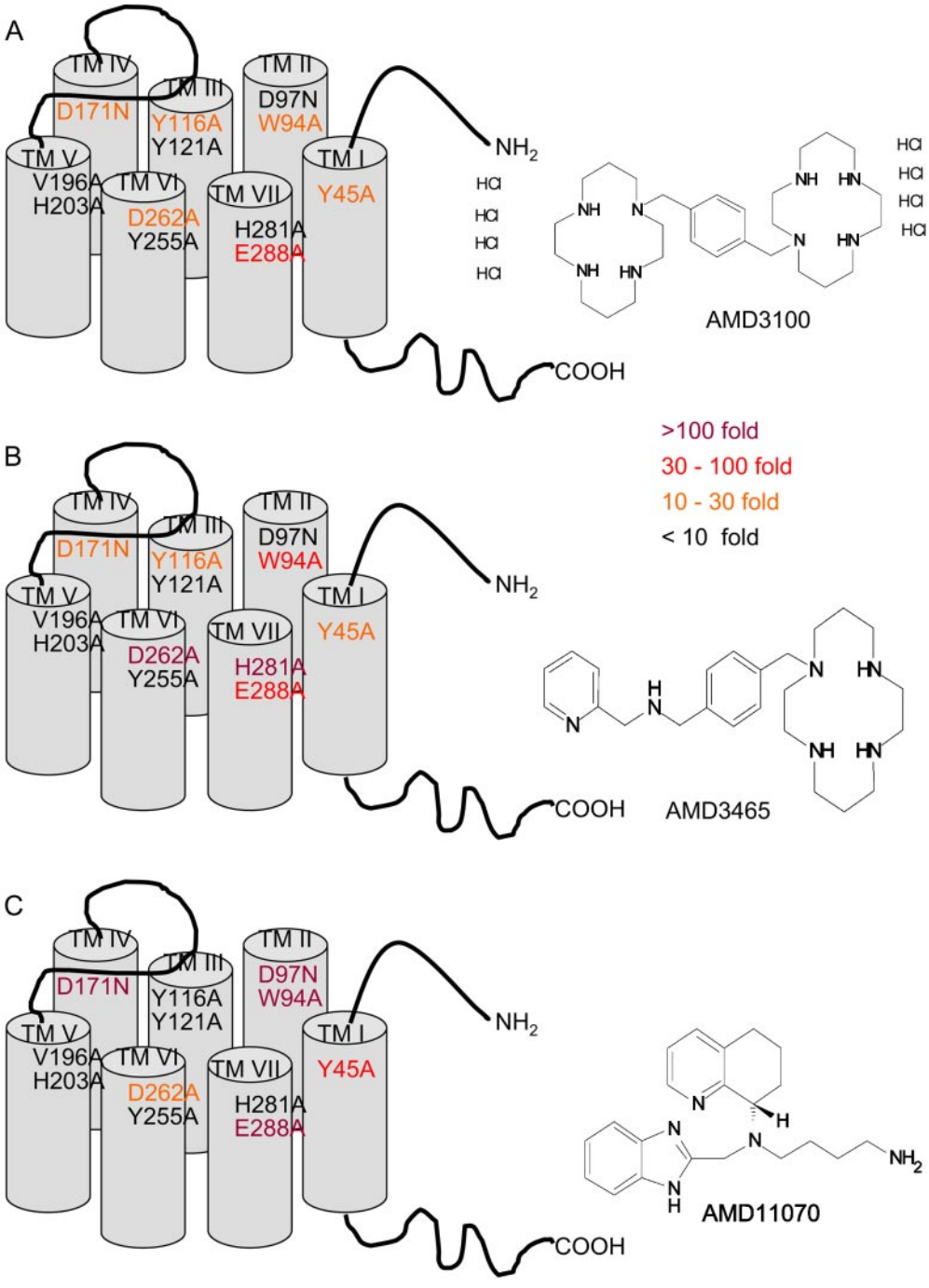


**Fig. 5.** Schematic diagram of the CXCR4 receptor depicting the effect of mutations on the interactions with CXCR4 inhibitors. A, AMD3100. B, AMD3465. C, AMD11070. For clarity, all the intracellular and extracellular loops except for ECLII are omitted. In addition, the mutations in ECLII, which did not affect the binding of any inhibitors, are not indicated. The levels of effect of each mutation on the $K_i$ values of the compounds in $^{125}$I-SDF-1$\alpha$ competitive binding are indicated by the following font color: purple, >100-fold increase in $K_i$ value; red, 30- to 100-fold increase in $K_i$ value; orange, 10- to 30-fold increase in $K_i$ value; and black, <10-fold increase in $K_i$ value.

sequently, because $Glu^{288}$ is positioned approximately two helical turns below $His^{281}$, an ionic interaction with the protonated dibenzyl-amine is possible. The double protonated cyclam ring of AMD3465 can then interact with $Trp^{94}$ (Fig. 6D), $Asp^{171}$ (Fig. 6E), or $Asp^{262}$ (Fig. 6F). In each case, there are amino acids residues that are not involved in direct small-molecule inhibitor-receptor interactions.

In the proposed binding modes for AMD11070 (Fig. 6, G–I), the double protonated molecule potentially could form ionic interactions with different negatively charged amino acids ($Asp^{97}$, $Asp^{171}$, $Asp^{262}$, and $Glu^{288}$). In Fig. 6G, the protonated primary amine forms an ionic hydrogen bond with $Asp^{97}$ and an additional cationic $\pi$-interaction with $Trp^{94}$. This binding model suggests that a hydrogen bond interaction could potentially be formed between $Tyr^{45}$ and benzimidazole of AMD11070, whereas $Glu^{288}$, $Asp^{171}$, and $Asp^{262}$ are not engaged in direct interactions with the inhibitor. In the second binding model (Fig. 6H), the primary amine of AMD11070 interacts with $Asp^{171}$, whereas the benzimidazole reaches into the pocket region defined by TMI, TMII, and TMVII and forms aromatic interactions with $Tyr^{45}$ and $Trp^{94}$. In the third binding mode (Fig. 6I), the primary amine interacts with $Asp^{262}$, and the protonated tertiary amine is able to approach $Glu^{288}$. Again, in each of these scenarios, some amino acid residues are not involved in direct interactions with the inhibitor.

## Discussion

The objective of this study is to understand the binding interactions of the small-molecule CXCR4 inhibitors with the receptor. All three compounds are selective inhibitors of CXCR4, inhibiting both SDF-1$\alpha$-dependent and -independent receptor interactions. Although there is evidence to suggest that AMD3100 may be a weak agonist, AMD3100 has been shown not to cause CXCR4-mediated calcium flux, G protein activation, and chemotaxis (Fricker et al., 2006), and neither AMD3100 nor AMD3465 cause CXCR4 receptor internalization (Hatse et al., 2002).

Nine single-site mutants of hCXCR4 were generated by site-directed mutagenesis for this study, and these mutants were used in combination with the five mutants, $Asp^{171}$, $Val^{196}$, $Asp^{262}$, $His^{281}$, and $Glu^{288}$, described previously (Gerlach et al., 2001). Residues $Asp^{97}$ and $Arg^{183}$ were investigated because they have been reported to be significant in the HIV-1 coreceptor function of CXCR4 (Brelot et al., 2000; Gerlach et al., 2001). Residues $Tyr^{45}$, $Trp^{94}$, $Tyr^{116}$, $Tyr^{121}$, and $His^{203}$ were chosen because their homologous residues in CCR5 have been shown to be involved in interactions with CCR5 receptor inhibitors (Dragic et al., 2000; Tsamis et al., 2003). $Tyr^{255}$, like some of the residues mentioned above ($Tyr^{45}$, $Trp^{94}$, and $Tyr^{121}$), has been suggested to be located in

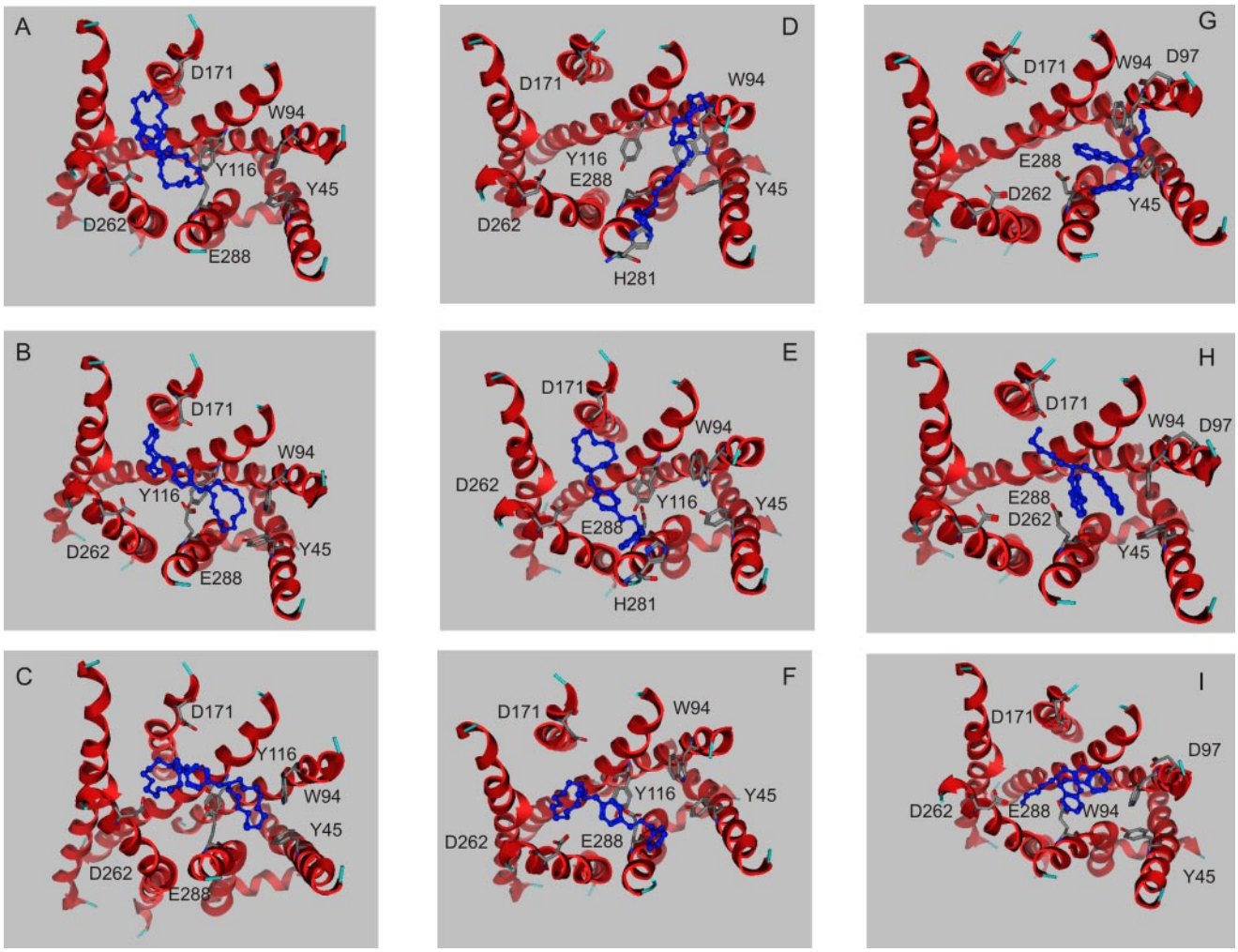


**Fig. 6.** Potential binding modes of AMD3100 (A–C), AMD3465 (D–F), and AMD11070 (G–I). Hydrogens are omitted for clarity.

the proposed hydrophobic binding pockets of CXCR4; therefore, it was of interest to investigate whether these residues, like their counterparts in CCR5, had similar effect on the binding of CXCR4 inhibitors (Huang et al., 2003). In addition, input from molecular modeling had suggested that $Asn^{176}$, as well as some of the above-mentioned residues, might potentially be involved in the binding with small-molecule inhibitors. All of the mutants demonstrated close to wild-type $K_d$ values in $^{125}$I-SDF-1$\alpha$ homologous competitive binding (Table 1), indicating that the mutations did not alter the affinity of SDF-1$\alpha$ for the receptor or significantly change the conformation of the receptor.

Some of the mutations affected the signaling response to SDF-1$\alpha$. This lack of response to SDF-1$\alpha$ could be due to reduced affinity of the mutated receptor for SDF-1$\alpha$, low expression of the mutated receptor, or changing an amino acid that is important in the signaling mechanism. The nonresponsiveness of the D97N and E288A mutants to SDF-1$\alpha$-induced calcium flux signaling has been reported previously (Brelot et al., 2000). It is noteworthy that, in the same study, both mutants were also impaired in SDF-1$\alpha$ binding, contrary to what we observed in our study. In our hands, all mutants demonstrated a very similar to wild-type affinity for SDF-1$\alpha$ in the $^{125}$I-SDF-1$\alpha$ competitive binding assay, suggesting that the SDF-1$\alpha$ binding affinity of these mutants were not affected. However, some mutants (W94A, D171N, D262N, and E288A) consistently demonstrated a reduced maximal $^{125}$I-SDF-1$\alpha$ binding compared with the wild type receptor, indicative of a lower level of expression (Table 2). These data therefore suggest that the attenuated signaling response of these mutant receptors might be due to low expression of the mutated receptor. Conversely, the other mutant receptors (Y45A, D97N, Y116A, Y255A, and H281A) exhibiting a low signaling response had comparable or higher expression than the wild-type receptor, suggesting that these residues may play a role in the signal transduction mechanism.

Several of the mutations had a profound effect on $K_i$ of the three inhibitors. The effect of mutations in TMIV to VII (D171N, H203A, D262N, H281A, and E288A) on the binding of AMD3100 had been reported previously (Gerlach et al., 2001; Rosenkilde et al., 2004). These studies used transient expression in COS-7 cells, and competitive binding with either radiolabeled monoclonal antibody 12G5 or met-SDF-1$\alpha$, whereas we used the natural ligand SDF-1. The effect of these mutations on AMD3100 inhibition was found to be very similar to our own observations, further validating our experimental system.

Most of the mutations in TMI, II, and III (Y45A, W94A, D97N and Y116A) were found to affect the binding of the CXCR4 inhibitors in this study. Like their counterparts in CCR5, the three conserved hydrophobic residues in the transmembrane regions, $Tyr^{45}$, $Trp^{94}$, and $Tyr^{116}$ ($Tyr^{37}$, $Trp^{86}$, and $Tyr^{108}$, respectively, in CCR5), might constitute a similar hydrophobic pocket that is involved in the binding of small-molecule inhibitors (Dragic et al., 2000; Tsamis et al., 2003).

Our results showed that the D97N mutation had a very significant impact on the binding of AMD11070 exclusively. Because AMD11070 is the only molecule that carries a primary amine, it is conceivable that the mutation abolished the potential electrostatic interactions between the primary amine moiety and the carboxylic acid group in the aspartic acid of the wild-type receptor. Given that $Asp^{97}$ is not conserved among chemokine receptors and is important for the HIV coreceptor function (Fig. 4) (Brelot et al., 2000), interactions with this residue can be further exploited for the design of specific CXCR4 antagonists for anti-HIV therapy.

$His^{281}$ is another amino acid residue that is unique in the CXCR4 sequence (Fig. 4) and affected the binding of AMD3465 exclusively in this study. This has been confirmed in a recent report (Rosenkilde et al., 2007). This additional interaction might enhance inhibitor binding to the receptor and therefore contribute to the higher potency of AMD3465 compared with AMD3100. Similar to a previous report (Hatse et al., 2001), we observed a slight increase (5-fold) in inhibitory activity of AMD3100 in the H281A mutant; the explanation or significance of this finding is not yet obvious.

In the current study, a homology model of CXCR4 derived from bovine rhodopsin is used as the working structural model to derive binding modes of small molecules. Despite low sequence identity between CXCR4 and bovine rhodopsin (approximately 23%), the validity of the crystal structure of bovine rhodopsin as a structural template for class A GPCRs has been critically assessed in the literature (Ballesteros and Palczewski, 2001; Ballesteros et al., 2001). Experimental methods such as creation of metal binding sites, disulfide cross-linking between close helices, and the substituted cysteine accessibility method have been used to establish that, despite low sequence identity among the members of class A GPCRs, there is a significant structural similarity within the transmembrane region. The recently published crystal structure of the $\beta$2-adrenergic receptor strongly supports this conclusion (Costanzi, 2008).

Despite this overall similar tertiary structure, which is also termed structural mimicry, local discrepancies between bovine rhodopsin and other class A members have been described previously (Ballesteros et al., 2001; Govaerts et al., 2001, 2003). Extensive experimental and computational studies have investigated the extracellular region of TM2 among class A GPCRs. The replacement of the GGF motif in TM2 of bovine rhodopsin by a TXP motif in chemokine receptors causes the extracellular end of TM2 to shift away from TM1 toward TM3, as well as the reorientation of residues such as $Trp^{94}$ in CXCR4 to point into the small-molecule binding site instead of the cell membrane. This reorientation of $Trp^{94}$ actually allows for a better explanation of the W94A mutant results obtained in this study. Other local inconsistencies between bovine rhodopsin and CXCR4 include the presence or absence of prolines, glycines, serines, threonines, and cysteines. These amino acids are known to create kinks in $\alpha$ helices. However, the evaluation of the CXCR4 homology models derived from the bovine rhodopsin coordinates did not require any additional adjustments in these regions.

Based on the experimental results the compounds had been manually docked into the putative binding site of hCXCR4. The proposed binding site is located in the extracellular transmembrane region beneath ECLII and extends over the whole cross-section of the receptor. Mutagenesis investigations in small-molecule binding to CCR2B and CCR5 have provided similar conclusions (Dragic et al., 2000; Berkhout et al., 2003; Tsamis et al., 2003; Nishikawa et al., 2005; Maeda et al., 2006; Seibert et al., 2006; Kondru et al., 2008). However, one key structural feature of the cyclam CXCR4 inhibitors is the potential for multiple ionic interactions, whereas the CCR5 inhibitors form

predominantly hydrophobic interactions with CCR5. Nevertheless, our data suggest that, like the CCR5 small-molecule inhibitors, these CXCR4 inhibitors mediate their effects by binding to the transmembrane regions of the receptor, which sequentially causes a conformational change leading to the disruption of receptor function.

It is of interest, however, that none of the small-molecule inhibitors studied here can be docked into CXCR4 and explain all mutant results by a direct ligand-receptor interaction. One possible reason is that there are indeed amino acid residues that interact with small-molecule inhibitors over a longer distance. For example, the substitution of charged amino acids may change the electrostatic nature of the binding pocket so that kinetic and thermodynamic contributions of small-molecule binding are altered. Alternatively, it is possible that small-molecule inhibitors can bind in several orientations to the receptor by directly interacting with different subsets of amino acid residues, and the results of mutagenesis reflect a timed average. We attempted to account for this mechanistic possibility by presenting several docking modes for each small-molecule inhibitor.

AMD3100 has been proposed to bind in an extended form to a binding pocket in the receptor constituted by TMIV, VI, and VII, with one cyclam binding to $Asp^{171}$ in TMIV and the second cyclam sandwiched between $Asp^{262}$ (TMVI) and $Glu^{288}$ (TMVII) (Gerlach et al., 2001). The other proposed AMD3100 binding mode had the positively charged bicyclam rings associated with $Asp^{262}$ and $Glu^{288}$ and the phenylenebis (methylene) linker associated with $Phe^{189}$ and $Tyr^{190}$ (Trent et al., 2003). A recent report suggested that the binding mode of AMD3465 seems to mimic that of AMD3100 but in a mode where the noncyclam moiety picks up additional interactions, especially with residues located more toward the extracellular end of TMVI and TMVII (e.g., $His^{281}$) (Rosenkilde et al., 2007). Although different assay systems were used, the binding interactions of AMD3100 and AMD3465 described here agree with those from previous reports (Gerlach et al., 2001; Hatse et al., 2001; Rosenkilde et al., 2007).

Our study compared the interactions of three structurally diverse small-molecule CXCR4 inhibitors with the receptor, including AMD11070, a first-in-class, orally bioavailable, noncyclam CXCR4 antagonist. We showed that these molecules interact with overlapping but not identical residues in the binding pocket of the receptor. To our knowledge, this is the first report of the molecular interactions of a noncyclam molecule with the receptor. We have identified an amino acid on the receptor, $Asp^{97}$, that is uniquely involved in the binding with AMD11070.

The additional binding sites identified for the monocyclam AMD3465 and for the nonmacrocyclic AMD11070 have extended our view of the receptor binding pocket. Furthermore, taking into account the proposed new interaction sites, molecular modeling suggested the possibility of multiple binding modes for each inhibitor. With the extended binding pocket, it might even be conceivable that two compounds can bind simultaneously to the inhibitor binding pocket. The heterologous competitive binding curves however, were all fitted to a single site binding molecule suggesting that only one inhibitor molecule binds to one receptor molecule. Based on our proposal of optional binding modes it would be interesting to further investigate the stoichiometry of inhibitor binding. These models suggest that the nonmacrocyclic AMD11070 can potentially have significantly different binding modes compared with the macrocyclic molecules. These mechanistic studies should prove to be useful for the development of future generations of CXCR4 inhibitors with improved clinical pharmacology and safety profiles.

**Acknowledgments**

We thank Gloria Lau, Vivian Law, Marilyn Darkes, and Stefan Idzan for technical assistance and Drs. M. Rosenkilde and T. Schwartz for providing CXCR4 mutants D171N, H203A, D262N, H281A and E288A.

**References**

Ballesteros J and Palczewski K (2001) G protein-coupled receptor drug discovery: implications from the crystal structure of rhodopsin. *Curr Opin Drug Discov Devel* **4:**561–574.

Ballesteros JA, Shi L, and Javitch JA (2001) Structural mimicry in G protein-coupled receptors: implications of the high-resolution structure of rhodopsin for structure-function analysis of rhodopsin-like receptors. *Mol Pharmacol* **60:**1–19.

Berkhout TA, Blaney FE, Bridges AM, Cooper DG, Forbes IT, Gribble AD, Groot PH, Hardy A, Ife RJ, Kaur R, et al. (2003) CCR2: characterization of the antagonist binding site from a combined receptor modeling/mutagenesis approach. *J Med Chem* **46:**4070–4086.

Birkenbach M, Josefsen K, Yalamanchili R, Lenoir G, and Kieff E (1993) Epstein-Barr virus-induced genes: first lymphocyte-specific G protein-coupled peptide receptors. *J Virol* **67:**2209–2220.

Brands JH, Maassen JA, van Hemert FJ, Amons R, and Möller W (1986) The primary structure of the alpha subunit of human elongation factor 1. Structural aspects of guanine-nucleotide-binding sites. *Eur J Biochem* **155:**167–171.

Brelot A, Heveker N, Montes M, and Alizon M (2000) Identification of residues of CXCR4 critical for human immunodeficiency virus coreceptor and chemokine receptor activities. *J Biol Chem* **275:**23736–23744.

Bridger GJ, Skerlj RT, Thornton D, Padmanabhan S, Martellucci SA, Henson GW, Abrams MJ, Yamamoto N, De Vreese K, and Pauwels R (1995) Synthesis and structure-activity relationships of phenylenebis(methylene)-linked bis-tetraazamacrocycles that inhibit HIV replication. Effects of macrocyclic ring size and substituents on the aromatic linker. *J Med Chem* **38:**366–378.

Burger JA and Kipps TJ (2006) CXCR4: a key receptor in the crosstalk between tumor cells and their microenvironment. *Blood* **107:**1761–1767.

Costanzi S (2008) On the applicability of GPCR homology models to computer-aided drug discovery: a comparison between in silico and crystal structures of the beta2-adrenergic receptor. *J Med Chem* **51:**2907–2914.

Dragic T, Trkola A, Thompson DA, Cormier EG, Kajumo FA, Maxwell E, Lin SW, Ying W, Smith SO, Sakmar TP, et al. (2000) A binding pocket for a small molecule inhibitor of HIV-1 entry within the transmembrane helices of CCR5. *Proc Natl Acad Sci U S A* **97:**5639–5644.

Flomenberg N, Devine SM, Dipersio JF, Liesveld JL, McCarty JM, Rowley SD, Vesole DH, Badel K, and Calandra G (2005) The use of AMD3100 plus G-CSF for autologous hematopoietic progenitor cell mobilization is superior to G-CSF alone. *Blood* **106:**1867–1874.

Freed EO, Myers DJ, and Risser R (1989) Mutational analysis of the cleavage sequence of the human immunodeficiency virus type 1 envelope glycoprotein precursor gp160. *J Virol* **63:**4670–4675.

Fricker SP, Anastassov V, Cox J, Darkes MC, Grujic O, Idzan SR, Labrecque J, Lau G, Mosi RM, Nelson KL, et al. (2006) Characterization of the molecular pharmacology of AMD3100: a specific antagonist of the G-protein coupled chemokine receptor, CXCR4. *Biochem Pharmacol* **72:**588–596.

Gerlach LO, Skerlj RT, Bridger GJ, and Schwartz TW (2001) Molecular interactions of cyclam and bicyclam non-peptide antagonists with the CXCR4 chemokine receptor. *J Biol Chem* **276:**14153–14160.

Govaerts C, Blanpain C, Deupi X, Ballet S, Ballesteros JA, Wodak SJ, Vassart G, Pardo L, and Parmentier M (2001) The TXP motif in the second transmembrane helix of CCR5. A structural determinant of chemokine-induced activation. *J Biol Chem* **276:**13217–13225.

Govaerts C, Bondue A, Springael JY, Olivella M, Deupi X, Le Poul E, Wodak SJ, Parmentier M, Pardo L, and Blanpain C (2003) Activation of CCR5 by chemokines involves an aromatic cluster between transmembrane helices 2 and 3. *J Biol Chem* **278:**1892–1903.

Hatse S, Princen K, Bridger G, De Clercq E, and Schols D (2002) Chemokine receptor inhibition by AMD3100 is strictly confined to CXCR4. *FEBS Lett* **527:**255–262.

Hatse S, Princen K, De Clercq E, Rosenkilde MM, Schwartz TW, Hernandez-Abad PE, Skerlj RT, Bridger GJ, and Schols D (2005) AMD3465, a monomacrocyclic CXCR4 antagonist and potent HIV entry inhibitor. *Biochem Pharmacol* **70:**752–761.

Hatse S, Princen K, Gerlach LO, Bridger G, Henson G, De Clercq E, Schwartz TW, and Schols D (2001) Mutation of Asp171 and Asp262 of the chemokine receptor CXCR4 impairs its coreceptor function for human immunodeficiency virus-1 entry and abrogates the antagonistic activity of AMD3100. *Mol Pharmacol* **60:**164–173.

Hendrix CW, Collier AC, Lederman MM, Schols D, Pollard RB, Brown S, Jackson JB, Coombs RW, Glesby MJ, Flexner CW, et al. (2004) Safety, pharmacokinetics, and antiviral activity of AMD3100, a selective CXCR4 receptor inhibitor, in HIV-1 infection. *J Acquir Immune Defic Syndr* **37:**1253–1262.

Hu JS, Freeman CM, Stolberg VR, Chiu BC, Bridger GJ, Fricker SP, Lukacs NW, and Chensue SW (2006) AMD3465, a novel CXCR4 receptor antagonist, abrogates

schistosomal antigen-elicited (type-2) pulmonary granuloma formation. *Am J Pathol* **169:**424–432.
Huang X, Shen J, Cui M, Shen L, Luo X, Ling K, Pei G, Jiang H, and Chen K (2003) Molecular dynamics simulations on SDF-1alpha: binding with CXCR4 receptor. *Biophys J* **84:**171–184.
Klabunde T and Hessler G (2002) Drug design strategies for targeting G-protein-coupled receptors. *Chembiochem* **3:**928–944.
Kondru R, Zhang J, Ji C, Mirzadegan T, Rotstein D, Sankuratri S, and Dioszegi M (2008) Molecular interactions of CCR5 with major classes of small-molecule anti-HIV CCR5 antagonists. *Mol Pharmacol* **73:**789–800.
Maeda K, Das D, Ogata-Aoki H, Nakata H, Miyakawa T, Tojo Y, Norman R, Takaoka Y, Ding J, Arnold GF, et al. (2006) Structural and molecular interactions of CCR5 inhibitors with CCR5. *J Biol Chem* **281:**12688–12698.
Marchese A, Heiber M, Nguyen T, Heng HH, Saldivia VR, Cheng R, Murphy PM, Tsui LC, Shi X, and Gregor P (1995) Cloning and chromosomal mapping of three novel genes, GPR9, GPR10, and GPR14, encoding receptors related to interleukin 8, neuropeptide Y, and somatostatin receptors. *Genomics* **29:**335–344.
Moore JP and Doms RW (2003) The entry of entry inhibitors: a fusion of science and medicine. *Proc Natl Acad Sci U S A* **100:**10598–10602.
Moyle G, DeJesus E, Boffito M, Wong R, Coakley E, Gibney C, Badel K, Calandra G, Bridger G, and Becker S (2007) CXCR4 antagonism: proof of activity with AMD11070, in *Proceedings of the 14th Conference on Retroviruses and Opportunistic Infections*; 2007 Feb 25–28; Los Angeles, CA. Abstract No. 511.
Murdoch C (2000) CXCR4: chemokine receptor extraordinaire. *Immunol Rev* **177:** 175–184.
Neote K, DiGregorio D, Mak JY, Horuk R, and Schall TJ (1993) Molecular cloning, functional expression, and signaling characteristics of a C-C chemokine receptor. *Cell* **72:**415–425.
Nishikawa M, Takashima K, Nishi T, Furuta RA, Kanzaki N, Yamamoto Y, and Fujisawa J (2005) Analysis of binding sites for the new small-molecule CCR5 antagonist TAK-220 on human CCR5. *Antimicrob Agents Chemother* **49:**4708–4715.
Oliveira L, Hulsen T, Lutje Hulsik D, Paiva AC, and Vriend G (2004) Heavier-than-air flying machines are impossible. *FEBS Lett* **564:**269–273.
Onuffer JJ and Horuk R (2002) Chemokines, chemokine receptors and small-molecule antagonists: recent developments. *Trends Pharmacol Sci* **23:**459–467.
Paterlini MG (2002) Structure modeling of the chemokine receptor CCR5: implications for ligand binding and selectivity. *Biophys J* **83:**3012–3031.
Power CA, Meyer A, Nemeth K, Bacon KB, Hoogewerf AJ, Proudfoot AE, and Wells TN (1995) Molecular cloning and functional expression of a novel CC chemokine receptor cDNA from a human basophilic cell line. *J Biol Chem* **270:**19495–19500.
Rosenkilde MM, Gerlach LO, Jakobsen JS, Skerlj RT, Bridger GJ, and Schwartz TW (2004) Molecular Mechanism of AMD3100 antagonism in the CXCR4 receptor: transfer of binding site to the cxcr3 receptor. *J Biol Chem* **279:**3033–3041.
Rosenkilde MM, Gerlach LO, Hatse S, Skerlj RT, Schols D, Bridger GJ, and Schwartz TW (2007) Molecular mechanism of action of monocyclam versus bicyclam non-peptide antagonists in the CXCR4 chemokine receptor. *J Biol Chem* **282:**27354–27365.
Saag MS, Rosenkrantz S, Becker S, Klingman K, Kallungal B, Zadzilka A, Coakley E, Acosta EP, Calandra G, and Team VAJftAAP (2007) Proof of concept of antiretroviral activity of AMD11070 (an orally administered CXCR4 entry inhibitor): results of the 1st dosing cohort A studied in NIH/NIAID AIDS Clinical Trials Group (ACTG) protocol A5210, in *Proceedings of the 14th Conference on Retroviruses and Opportunistic Infections*; 2007 Feb 25–28; Los Angeles, CA. Abstract no. 512.
Schols D, Claes S, Hatse S, Princen K, Vermeire K, Clercq ED, Skerlj R, Bridger G, and Calandra G (2003) Anti-HIV activity profile of AMD070, an orally bioavailable CXCR4 antagonist, in 10th *Conference on Retroviruses and Opportunistic Infections*; 2003 Feb 10–14; Boston, MA. Abstract no. 563.
Seibert C, Ying W, Gavrilov S, Tsamis F, Kuhmann SE, Palani A, Tagat JR, Clader JW, McCombie SW, Baroudy BM, et al. (2006) Interaction of small molecule inhibitors of HIV-1 entry with CCR5. *Virology* **349:**41–54.
Teller DC, Okada T, Behnke CA, Palczewski K, and Stenkamp RE (2001) Advances in determination of a high-resolution three-dimensional structure of rhodopsin, a model of G-protein-coupled receptors (GPCRs). *Biochemistry* **40:**7761–7772.
Trent JO, Wang ZX, Murray JL, Shao W, Tamamura H, Fujii N, and Peiper SC (2003) Lipid bilayer simulations of CXCR4 with inverse agonists and weak partial agonists. *J Biol Chem* **278:**47136–47144.
Tsamis F, Gavrilov S, Kajumo F, Seibert C, Kuhmann S, Ketas T, Trkola A, Palani A, Clader JW, Tagat JR, et al. (2003) Analysis of the mechanism by which the small-molecule CCR5 antagonists SCH-351125 and SCH-350581 inhibit human immunodeficiency virus type 1 entry. *J Virol* **77:**5201–5208.
Wegner SA, Ehrenberg PK, Chang G, Dayhoff DE, Sleeker AL, and Michael NL (1998) Genomic organization and functional characterization of the chemokine receptor CXCR4, a major entry co-receptor for human immunodeficiency virus type 1. *J Biol Chem* **273:**4754–4760.
Wong LM, Myers SJ, Tsou CL, Gosling J, Arai H, and Charo IF (1997) Organization and differential expression of the human monocyte chemoattractant protein 1 receptor gene. Evidence for the role of the carboxyl-terminal tail in receptor trafficking. *J Biol Chem* **272:**1038–1045.

**Address correspondence to:** Dr. Simon P. Fricker, 49 New York Ave., Framingham, MA 01701. E-mail: simon.fricker@genzyme.com